Current Research in Food Science 4 (2021) 287–294

Contents lists available at ScienceDirect

Current Research in Food Science

journal homepage: www.editorialmanager.com/crfs/

Research Paper

Identification of the Maillard reaction intermediates as divalent iron complexes in alanine/glucose/$FeCl_2$ model system using ESI/qTOF/MS/MS and isotope labelling technique

Eun Sil Kim, Varoujan Yaylayan *

Department of Food Science and Agricultural Chemistry, McGill University, 21111 Lakeshore, Ste Anne de Bellevue, Quebec, H9X 3V9, Canada

ARTICLE INFO

handling editor

Keywords:
Amadori rearrangement products
Maillard reaction intermediates
Metal complex
Sugar degradation products
Isotope labelling
ESI/qTOF/MS

ABSTRACT

Due to their high reactivities and short half-lives, the detection of Maillard reaction intermediates is relatively difficult to achieve in a single analytical run. In this study, the formation of Maillard reaction intermediates from heated alanine/glucose mixtures (110 °C for 2 h) was investigated through their complexation with divalent iron using electrospray ionization/quadrupole time-of-flight mass spectrometry and isotope labeling techniques. Analysis of the mixtures indicated that this approach allows the simultaneous detection of many important labile and reactive Maillard reaction intermediates along with unreacted alanine and glucose in addition to various other Maillard reaction products, such as glyceraldehyde, erythrose, ribose, acetol, glycolaldehyde, fructosamine, glucosone, osones, deoxyosones, and Amadori products. Some osones and deoxyosones also formed their corresponding Schiff bases with alanine. The above mentioned Maillard reactions intermediates were detected either as binary metal complexes with alanine or with other enediol generating species including self-complexation adducts and they formed positively charged ions such as $[M + H]^+$, $[M + Na]^+$, $[M + K]^+$, $[M + Fe^{35}Cl]^+$, and $[M + Fe^{37}Cl]^+$, that can be detected using the positive ionization mode.

1. Introduction

In the thermal processing of food, Maillard reaction intermediates (MRIs), resulting from the degradation of sugars and Amadori rearrangement products (ARPs) are considered important precursors for the development of color, flavor, and thermally generated toxicants (Yaylayan, 1997). Analysis of the MRIs and sugar degradation products (SDPs) has been achieved through the use of a range of time-consuming analytical technique (Yaylayan and Huyghues-Despointes, 1994; Davidek et al., 2002; Gensberger et al., 2013) that required elaborate procedures. Thus, various systems have been developed for the discrimination and determination of MRIs and ARPs. For example, volatile Maillard reaction products, including ARPs were analyzed by gas chromatography (GC) after derivatization step; however, this system has achieved limited success in analysis of the MRIs and their degradation products due to their low volatility (Yaylayan and Huyghues-Despointes, 1994). High-performance liquid chromatography (HPLC) and high-performance anion-exchange chromatography (HPAEC) based methods reported in the literature (Davidek et al., 2002; Gensberger et al., 2013) have been focused on the detection of nonvolatile water-soluble compounds of the Maillard products by using either refractive index or UV detection (Davidek et al., 2002; Gensberger et al., 2013). However, chemical derivatization steps (Davidek et al., 2002; Gensberger et al., 2013; Page et al., 1982) are essential for their analysis. Infrared (IR) spectroscopy was applied to quantify the open chain or *keto* forms of ARPs (Tamic and Hartman, 1983). In addition, Fourier transformed infrared (FTIR) spectroscopy has provided a more useful method to study the effect of environmental factors, such as pH and temperature, on the concentration of the *keto* form (Wnorowski and Yaylayan, 2003). Furthermore, nuclear magnetic resonance (NMR) spectroscopy, including 1D-^{1}H NMR, ^{13}C-NMR, DEPT-2D ^{1}H–^{1}H and ^{13}C–^{1}H correlational spectroscopy (COSY), and 2D nuclear Overhauser enhancement spectroscopy (NOESY) has also been employed for structural elucidation of the ARPs (Li et al., 2014; Kaufmann et al., 2016).

Abbreviations: ARPs, Amadori rearrangement products; 3-DG, 3-deoxyglucosone; ESI/qTOF/MS, Electrospray ionization/quadrupole time-of-flight mass spectrometry; HMF, Hydroxymethylfurfural; HPAEC, high-performance anion-exchange chromatography; GC, Gas chromatography; IR, Infrared; MRIs, Maillard Reaction Intermediates; MRM, Multiple reaction monitoring; NMR, Nuclear magnetic resonance; SDPs, Sugar degradation products.

* Corresponding author.
E-mail address: varoujan.yaylayan@mcgill.ca (V. Yaylayan).

https://doi.org/10.1016/j.crfs.2021.04.003
Received 5 March 2021; Received in revised form 7 April 2021; Accepted 8 April 2021

However, rapid analytical procedures for the simultaneous profiling of MRIs and SDPs have yet to be reported in the literature. In a previous study (Kim and Yaylayan, 2020), a convenient analytical procedure for profiling of SDPs through complexation with divalent metal ions combined with ESI/qTOF/MS was developed and applied for the analysis of honey. Here we demonstrate the utility of this technique to detect iron (II) catalyzed Maillard reaction intermediates of alanine and glucose using a methodology that most researchers already utilize, the qTOF/LC/MS with additional step of adding metal salts to the solution being analyzed. This step facilitates the detection of not only hard-to-identify and labile products but at the same time enhances the detection of nitrogen containing MRIs due to the ability metal ions to coordinate equally with nitrogen and oxygen atoms.

2. Materials and methods

2.1. Materials and reagents

L-alanine (98%), D-glucose, copper(II) chloride ($CuCl_2$) (99.9%) and iron(II) chloride ($FeCl_2$) (99%) were purchased from Sigma-Aldrich Chemical Co. (Oakville, Ontario, Canada). Alanine-3-^{13}C ($^{13}CH_3CH(NH_2)CO_2H$) (98%) and glucose ^{13}C–U ($^{13}C_6H_{12}O_6$) (99%) were purchased from Cambridge Isotope Laboratories (Andover, MI). Liquid chromatography-mass spectrometry (LC-MS)-grade water and methanol (OmniSolv, > 99%) were obtained from VWR International (Mississauga, Ontario, Canada).

2.2. Sample preparation

Test model systems were prepared by heating glucose (18 mg), alanine (9 mg), and $FeCl_2$ (6.4 mg) in methanol or water (1 mL) in tightly closed stainless-steel reactors at 110 °C for 2 h. Control model systems were prepared by heating glucose (18 mg) and alanine (9 mg) with or without $CuCl_2$ (5.6 mg) in methanol at 110 °C for 2 h. All samples were analyzed at least in two replicates, as indicated in Table 1.

2.3. ESI/qTOF/MS

The dry reaction mixtures were dissolved in liquid chromatography (LC)-grade methanol to a concentration of 1 mg/mL. The samples were then diluted 10-fold in 10% methanol prior to analysis by ESI/qTOF/MS in positive mode. The ESI/qTOF/MS system was comprised of a Bruker Maxis Impact quadrupole-time-of-flight mass spectrometer (Bruker Daltonics, Bremen, Germany) operated in positive-ion mode. Samples (1 μL) were injected directly into ESI/qTOF/MS. Instrument calibration was performed using sodium formate clusters. The electrospray interface settings were the following: nebulizer pressure, 0.6 bar; drying gas, 4 L/min; temperature, 180 °C; and capillary voltage, 4500 V. The scan range was from *m/z* 90 to 1000. Molecular formulae were assigned to all the observed peaks based on their exact *m/z* values by using the online software "ChemCalc" (Institute of Chemical Sciences and Engineering, Lausanne, Switzerland) (Patiny and Borel, 2013). ESI/qTOF/MS/MS was carried out in the multiple reaction monitoring (MRM) mode using a collision energy of 10.0 eV for the ions at *m/z* 252, 342, and 395.

Table 1
Composition of the model systems[a].

Model System	
Control Model System	Alanine was added to glucose solution and heated in the absence of metal ions - Ala/Glu
Test Model System	Alanine was added to glucose solution and heated in the presence of $CuCl_2$ - Ala/Glu/$CuCl_2$
Isotope Labelling Model System	Alanine was added to glucose^{13}C–U solution and heated in the presence of $FeCl_2$ - **Ala/Glu [^{13}C–U] /$FeCl_2$**
	Alanine-3-^{13}C was added to glucose solution and heated in the presence of $FeCl_2$ -**Ala [^{13}C-3] /Glu/$FeCl_2$**

[a] All the Model systems were prepared in 1:1 M ratio and heated at 110 °C for 2 h in water or methanol by using a sealed stainless-steel reactor and analyzed in at least two replicates.

2.4. Structural elucidation

Evidence for the proposed structures was provided through ESI/qTOF/MS analysis of their elemental composition, MS/MS analysis, and isotope-labeling. Furthermore, the incorporation of chlorine and copper in the identified complexes was also confirmed through the detection of their specific isotopic signatures; for chlorine the [M + 2] peaks accounted for ~ 25% of the peak intensity for the M ions, while for copper, the [M + 2] peaks accounted for ~ 30% of the peak intensity. Isotope labelling techniques was also used to generate the corresponding isotopically-labelled counterparts from [^{13}C–U]-labelled glucose and [^{13}C-3]-labelled alanine. The proposed structures represent only one possible isomeric form out of many possible forms for a particular nominal molecular weight, and are based on the most commonly reported structures in the literature.

3. Results and discussion

Sugar degradation products formed during the Maillard reaction are normally more amenable for analysis under negative ionization mode when analyzed by mass spectrometry (Figure S1). However, the addition of metal ions prior to analysis allows these mixtures to be analyzed in the positive ionization mode (Kim and Yaylayan, 2020), where nitrogen-containing MRPs are also readily detectable (Figure S2). Furthermore, the formation of metal complexes can prevent the degradation or further reactions of these reactive intermediates, while at the same time providing structural features for the development of the positive charge necessary for their detection under the positive ionization mode of the ESI/qTOF/MS system (Kim and Yaylayan, 2020). In the presence of metal ions, sugars, amino acids, MRIs (i.e., ARPs), and SDPs (i.e., 3-deoxyglucosone (3-DG), α-hydroxyl carbonyl, and α-dicarbonyl compounds) have the ability to undergo self- or random complexation to generate various metal-centered binary complexes, as listed in Table 2. In this study, the alanine/glucose model system was heated at 110 °C for 2 h in the presence of metal ions ($FeCl_2$ or $CuCl_2$) in water or methanol, and analyzed by ESI/qTOF/MS in the positive ionization mode. The heating of glucose and alanine in the absence of metal ions was also performed as a control, and it was found that the control system also produced alanine Amadori compound with glucose as the dominant product, but with reduced formation of other MRPs, as analyzed under positive ionization mode.

3.1. Identification of the Maillard reaction intermediates through complexation with Iron(II) using ESI/qTOF/MS and ESI/qTOF/MS/MS analysis

The Maillard reaction intermediates obtained (see Tables S1 and S2) in all the model systems heated at 110 °C for 2 h could be categorized into four groups **(1)** metal complexes with free amino acids/and or intact sugars, **(2)** ARPs and their corresponding metal complexes, **(3)** amino sugars and their corresponding metal complexes, and **(4)** reactive SDPs and their metal complexes. Table 2 shows selected examples of the above complexes. Previously (Kim and Yaylayan, 2020), we demonstrated that SDPs acting as bidentate ligands were converted into stable metal complexes, and were easily profiled by ESI/qTOF/MS in the positive ionization mode. In this study, the alanine/glucose model system was reacted in the presence or absence of $FeCl_2$ or $CuCl_2$ as metal catalysts to enhance the formation of MRPs, and at the same time to provide the metal ions needed for the formation of stable binary complexes for detection by ESI/qTOF/MS in positive ionization mode.

Table 2
Possible binary complexes of divalent metal ions with Maillard reaction precursors and intermediates.[a]

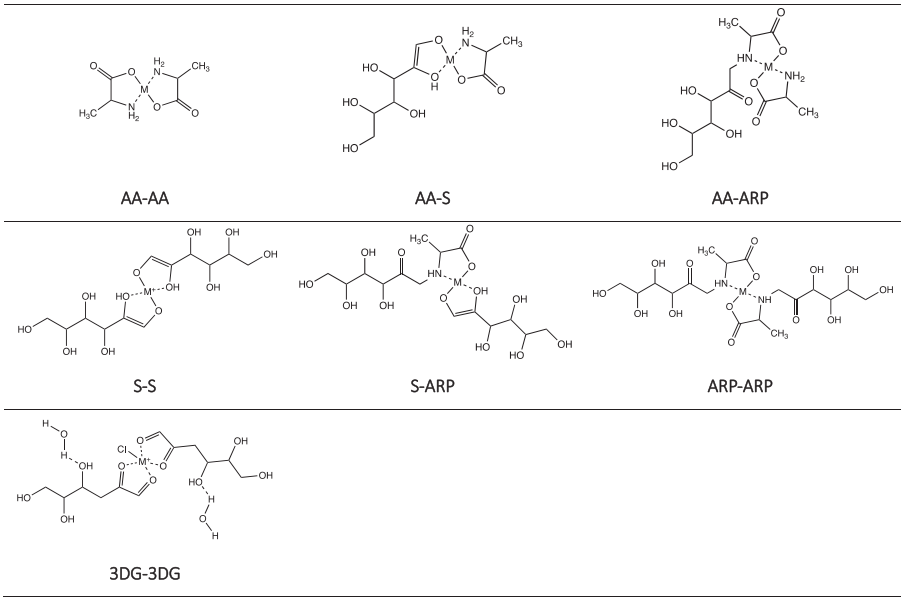

3.1.1. Detection of intact amino acid and intact sugar metal complexes

The amino acid metal complexes were detected as mono(alaninate)- and *bis*(alaninato)iron(II) complexes and were observed as $[M]^+$ ions at *m/z* values of 143.9744 ($C_3H_6FeNO_2$) and 233.0224 ($C_6H_{13}FeN_2O_4$), respectively. These structures were confirmed by observing the incorporation of one or two carbon atoms from [^{13}C-3] alanine, but no carbon atoms from [^{13}C–U] glucose. Furthermore, mono(alaninate)iron(II) was found to conjugate with glucose to give a signal as $[M + H]^+$ at *m/z* 324.0378 ($C_9H_{18}FeNO_8$) that was found to incorporate six carbon atoms from [^{13}C–U] glucose and one C-3 atom from [^{13}C-3] alanine. The ions corresponding to the free alanine or glucose were observed as $[M + H]^+$ ions at *m/z* 90.055 ($C_3H_9NO_2$) or $[M + K]^+$ ions at *m/z* 219.0266 ($C_6H_{12}KO_6$) not shown in Tables 2 and S1.

3.1.2. Detection of Amadori rearrangement products

The Amadori product of alanine with glucose, namely *N*-(1-deoxy-D-fructose-1-yl)-L-alanine, was observed as the dominant peak in both the Ala/Glu and the Ala/Glu/$FeCl_2$ model systems, being detected in its free form $[M]^+$ at *m/z* 252.1074 ($C_9H_{18}NO_7$). It was also detected as $[M + Na]^+$ at *m/z* 274.0891 ($C_9H_{17}NNaO_7$) and $[M + K]^+$ at *m/z* 290.0662 ($C_9H_{17}NKO_7$). All structures were confirmed by observing the incorporation of six carbon atoms from [^{13}C–U] glucose and one C-3 atom from [^{13}C-3] alanine. The Amadori product was observed to undergo three dehydration reactions generating $[M - H_2O]^+$ at *m/z* 234.0967 ($C_9H_{16}NO_6$) and $[M - 2H_2O]^+$ at *m/z* 216.0863 ($C_9H_{14}NO_5$), and $[M - 3H_2O]^+$ at *m/z* 198.0755 ($C_9H_{12}NO_4$). In addition, the hydrated form $[M + H_2O]^+$ appeared at *m/z* 270.1175 ($C_9H_{20}NO_8$). All three dehydrated ions and the hydrated ion were found to incorporate six carbon atoms from [^{13}C–U] glucose and one carbon atom from [^{13}C-3] alanine. Furthermore, the ARP was also observed as a *bis*-ARP iron(II) complex as $[M + H]^+$ at *m/z* 557.1295 ($C_{18}H_{33}FeN_2O_{14}$), where twelve carbon atoms from glucose and two C-3 atoms from alanine were incorporated in the structure. In addition, the ARP was able to form iron complexes with alanine at *m/z* 395.0752 ($C_{12}H_{23}FeN_2O_9$) and with glucose at *m/z* 486.0917 ($C_{15}H_{28}FeNO_{13}$), wherein the former was confirmed by detecting the incorporation of six carbons from [^{13}C–U] glucose and two C-3 atoms from [^{13}C-3] alanine, while the latter contained twelve carbon atoms from [^{13}C–U] glucose and one C-3 atoms from [^{13}C-3] alanine (see Tables S1 and 2). In methanol, the methyl ester of the ARP was also observed as the second dominant peak in the form of $[M + H]^+$ at *m/z* 266.1229 (C10H20NO7), as well as $[M + Na]^+$ at *m/z* 288.1059 ($C_{10}H_{19}NNaO_7$). These structures were confirmed by observing the incorporation of six carbon atoms from [^{13}C–U] glucose and one C-3 atom from [^{13}C-3] alanine, respectively. Dehydrated ARP esters were detected as $[M + H - H_2O]^+$ at *m/z* 248.1125 ($C_{10}H_{18}NO_6$) and $[M + H - 2H_2O]^+$ at *m/z* 230.1019 ($C_{10}H_{16}NO_5$) (see Tables 3 and S1). Both dehydrated ions were found to incorporate six carbon atoms from [^{13}C–U] glucose and one carbon atom from [^{13}C-3] alanine.

In addition to glucose, smaller sugars, such as glycolaldehyde, glyceraldehyde, and erythrose were also found to form Amadori products with alanine as either free or as mono(alaninato)iron(II) complexes. More specifically, the free glycolaldehyde Amadori compound was observed as $[M + H]^+$ at *m/z* 132.0656 ($C_5H_{10}NO_3$) and the iron complex was observed as $[M]^+$ at *m/z* 185.9848 ($C_5H_8FeNO_3$). Both structures incorporated two carbon atoms from glucose and one C-3 atom from alanine. Similarly, the glyceraldehyde and acetol Amadori compounds of mono(alaninate)iron(II) were observed at *m/z* 215.9958 ($C_6H_{10}FeNO_4$) and *m/z* 200.001 ($C_6H_{10}FeNO_3$), respectively, where three carbon atoms from glucose and one C-3 atom from alanine were incorporated in both structures. Moreover, the erythrose Amadori compound of alanine was also observed at *m/z* 246.0064 ($C_7H_{12}FeNO_5$), which was found to incorporate four carbon atoms from glucose and one C-3 atom from alanine. Interestingly, 3-deoxyerythrosone was observed as the mono(-alaninate)iron(II) complex of its Schiff base as $[M]^+$ at *m/z* 227.9968 ($C_7H_{10}FeNO_4$), whereas, 3-deoxyerythrose was observed at *m/z* 230.0117 ($C_7H_{12}FeNO_4$) most likely as the Amadori compound. These structures were confirmed by detecting the incorporation of four carbon atoms from [^{13}C–U] glucose and one C-3 atom from [^{13}C-3] alanine. Similar to the case of 3-deoxyerythrosone, glycerosone (hydroxymethylglyoxal) was also observed as the mono(alaninato)iron(II) complex of its Schiff base at *m/z* 231.9913 ($C_6H_{10}FeNO_5$), where three carbon atoms from glucose and one C-3 atom from alanine were found incorporated. Furthermore, the Schiff base of glucosone with methyl ester of alanine was detected as $[M + H]^+$ at *m/z* 264.1085 ($C_{10}H_{18}NO_7$) along with its dehydrated form $[M + H - H_2O]^+$ at *m/z* 246.0979 ($C_{10}H_{16}NO_6$). Both structures incorporated six carbon atoms from glucose and one C-3 atom from alanine.

Table 3
Elemental composition and/or isotope incorporation of the common Maillard reaction intermediates obtained in the Ala/Glu/$CuCl_2$, and Ala/Glu/$FeCl_2$ model system in methanol (see Table S1).

Ala/Glu/$CuCl_2$			Ala/Glu/$FeCl_2$			Ala/Glu[^{13}C–U]/$FeCl_2$			Ala[^{13}C-3]/Glu/$FeCl_2$		
[M + X]	Elemental Composition[a]	Error PPM[b]	[M + X]	Elemental Composition	Error PPM	[M + X]	Elemental Composition	Error PPM	[M + X]	Elemental Composition	Error PPM
127.0386	$C_6H_7O_3$	7.235	127.0389	$C_6H_7O_3$	4.873	133.0585	$[^{13}C]_6H7O_3$	8.629	127.0384	$C_6H_7O_3$	8.809
nd[c]			143.9744	$C_3H_6FeNO_2$	2.747	143.9741	$C_3H_6FeNO_2$	4.831	144.9769	$C_2[^{13}C]H_6FeNO_2$	8.625
180.0862	$C_6H_{14}NO_5$	5.539	180.0867	$C_6H_{14}NO_5$	2.763	186.1058	$[^{13}C]_6H_{14}NO_5$	8.203	180.0857	$C_6H_{14}NO_5$	8.316
162.0757	$C_6H_{12}NO_4$	5.756	162.0761	$C_6H_{12}NO_4$	2.671	168.0952	$[^{13}C]_6H_{12}NO_4$	9.292	162.0751	$C_6H_{12}NO_4$	9.458
144.0645	$C_6H_{10}NO_3$	10.885	144.0656	$C_6H_{10}NO_3$	4.638	150.085	$[^{13}C]_6H_{10}NO_3$	7.977	144.0644	$C_6H_{10}NO_3$	11.579
126.0545	$C_6H_8NO_2$	7.961	126.0543	$C_6H_8NO_2$	3.994	132.0751	$[^{13}C]_6H_8NO_2$	4.032	126.0544	$C_6H_8NO_2$	8.754
202.0701	$C_6H_{13}NNaO_5$	4.74	202.071	$C_6H_{13}NNaO_5$	9.194	nd			202.068	$C_6H_{13}NNaO_5$	5.653
206.1018	$C_8H_{16}NO_5$	5.083	206.102	$C_8H_{16}NO_5$	4.113	212.1201	$C_2[^{13}C]_6H_{16}NO_5$	13.56	207.1042	$C_7[^{13}C]H_{16}NO_5$	9.669
188.0914	$C_8H_{14}NO_4$	4.694	188.0917	$C_8H_{14}NO_4$	3.099	194.1109	$C_2[^{13}C]_6H_{14}NO_4$	7.789	189.0939	$C_7[^{13}C]H_{14}NO_4$	9.19
240.0159	$C_6H_{13}[^{63}Cu]N_2O4$	5.137	233.0224	$C_6H_{13}FeN_2O_4$	0.318	233.0205	$C_6H_{13}FeN_2O_4$	8.471	235.0253	$C_4[^{13}C]_2H_{13}FeN_2O_4$	16.524
242.013	$C_6H_{13}[^{65}Cu]N_2O_4$[d]	9.609	na[e]			na			na		
nd			234.9907	$C_6H_{11}FeO_6$	0.85	241.0089	$[^{13}C]_6H_{11}FeO_6$	7.196	234.9897	$C_6H_{11}FeO_6$	3.427
nd			216.9802	$C_6H_9FeO_5$	1.196	222.9981	$[^{13}C]_6H_9FeO_5$	8.832	nd		
nd			198.9686	$C_6H_7FeO_4$	3.899	204.9872	$[^{13}C]_6H_7FeO_4$	11.24	198.9668	$C_6H_7FeO_4$	12.946
nd			270.9673	$C_6H_{12}[^{35}Cl]FeO_6$	0.45	276.9861	$[^{13}C]_6H_{12}[^{35}Cl]FeO_6$	4.157	270.9652	$C_6H_{12}[^{35}Cl]FeO_6$	−7.3
nd			272.9646	$C_6H_{12}[^{37}Cl]FeO_6$[f]	1.37	278.983	$[^{13}C]_6H_{12}[^{37}Cl]FeO_6$	− 4.86	272.9629	$C_6H_{12}[^{37}Cl]FeO_6$	−4.86
252.1074	$C_9H_{18}NO_7$	3.677	252.1082	$C_9H_{18}NO_7$	1.297	258.1266	$C_3[^{13}C]_6H_{18}NO_7$	7.19	253.1099	$C_8[^{13}C]H_{18}NO_7$	7.039
234.0967	$C_9H_{16}NO_6$	4.538	234.0976	$C_9H_{16}NO_6$	1.547	240.1161	$C_3[^{13}C]_6H_{16}NO_6$	7.46	235.0994	$C_8[^{13}C]H_{16}NO_6$	7.304
216.0863	$C_9H_{14}NO_5$	4.154	216.087	$C_9H_{14}NO_5$	1.84	222.1056	$C_3[^{13}C]_6H_{14}NO_6$	7.774	nd[c]		
198.0755	$C_9H_{12}NO_4$	5.719	198.0765	$C_9H_{12}NO_4$	1.68	204.0963	$C_3[^{13}C]_6H_{12}NO_4$	2.263	199.077	$C_8[^{13}C]H_{12}NO_4$	15.008
270.1175	$C_9H_{20}NO_8$	5.152	270.1188	$C_9H_{20}NO_8$	1.08	296.0822	$C_3[^{13}C]_6H_{20}NO_8$	7.22	271.1204	$C_8[^{13}C]H_{20}NO_8$	6.81
274.0891	$C_9H_{17}NNaO_7$	4.274	274.0908	$C_9H_{17}NNaO_7$	0.626	276.1391	$C_3[^{13}C]_6H_{17}NnaO_7$	0.287	275.0087	$C_8[^{13}C]H_{17}NnaO_7$	7.366
290.0662	$C_9H_{17}KNO_7$	6.865	290.0673	$C_9H_{17}KNO_7$	10.657	280.1084	$C_3[^{13}C]_6H_{17}NKO_7$	7.142	291.0641	$C_8[^{13}C]H_{17}NKO_7$	11.9
266.1229	$C_{10}H_{20}NO_7$	4.047	266.1237	$C_{10}H_{20}NO_7$	1.041	272.1423	$C_4[^{13}C]_6H_{20}NO_7$	6.636	267.1255	$C_9[^{13}C]H_{20}NO_7$	6.858
248.1125	$C_{10}H_{18}NO_6$	3.677	248.1132	$C_{10}H_{18}NO_6$	0.856	nd			249.115	$C_9[^{13}C]H_{18}NO_6$	7.094
230.1019	$C_{10}H_{16}NO_5$	4.118	230.1026	$C_{10}H_{16}NO_5$	1.076	236.1213	$C_4[^{13}C]_6H_{16}NO_5$	7.101	231.1046	$C_9[^{13}C]H_{16}NO_5$	6.934
288.1059	$C_{10}H_{19}NNaO_7$	0.075	288.1071	$C_{10}H_{19}NNaO_7$	4.09	294.1239	$C_4[^{13}C]_6H_{19}NnaO_7$	7.312	289.1074	$C_9[^{13}C]H_{19}NnaO_7$	6.491
nd			284.9825	$C_7H_{14}[^{35}Cl]FeO_6$	−1.15	291.0013	$C[^{13}C]_6H_{14}[^{35}Cl]O_6$	− 5.69	284.9819	$C_7H_{14}ClFeO_6$	−3.25
nd			286.9816	$C_7H_{14}[^{37}Cl]FeO_6$	6	nd			nd		
331.0317	$C_9H_{18}[^{63}Cu]NO_8$	3.452	324.0378	$C_9H_{18}FeNO_8$	1.184	330.0561	$C_3[^{13}C]_6H_{18}FeNO_8$	6.704	325.0384	$C_8[^{13}C]H_{18}FeNO_8$	9.656
333.0304	$C_9H_{18}[^{65}Cu]NO_8$	− 1.9	na			na			na		
360.1468	$C_{12}H_{26}NO_{11}$	10.511	360.1503	$C_{12}H_{26}NO_{11}$	0.793	372.1868	$[^{13}C]_{12}H_{26}NO_{11}$	10.87	360.1483	$C_{12}H_{26}NO_{11}$	6.346
342.1387	$C_{12}H_{24}NO_{10}$	3.861	342.14	$C_{12}H_{24}NO_{10}$	0.061	354.1779	$[^{13}C]_{12}H_{24}NO_{10}$	6.717	342.1381	$C_{12}H_{24}NO_{10}$	5.615
324.1281	$C_{12}H_{22}NO_9$	4.184	324.1292	$C_{12}H_{22}NO_9$	0.791	336.1675	$[^{13}C]_{12}H_{22}NO_8$	6.587	324.1275	$C_{12}H_{22}NO_9$	6.036
306.1176	$C_{12}H_{20}NO_8$	4.219	306.1188	$C_{12}H_{20}NO_8$	0.299	318.157	$[^{13}C]_{12}H_{20}NO_7$	6.757	306.1172	$C_{12}H_{20}NO_8$	5.526
nd			288.107	$C_{12}H_{18}NO_7$	4.606	300.1432	$[^{13}C]_{12}H_{18}NO_6$	17.94	288.1051	$C_{12}H_{18}NO_7$	11.2
402.0686	$C_{12}H_{23}[^{63}Cu]N_2O_9$	3.374	395.0752	$C_{12}H_{23}FeN_2O_9$	0.247	401.0928	$C_6[^{13}C]_6H_{23}FeN_2O_9$	6.548	397.0789	$C_{10}[^{13}C]_2H_{23}FeN_2O_9$	7.825
386.058	$C_{12}H_{21}[^{65}Cu]N_2O_8$	1.09	na			na			na		
424.0504	$C_{12}H_{22}[^{63}Cu]N_2NaO_9$	3.54	417.0581	$C_{12}H_{22}FeN_2NaO_9$	2.057	nd			419.0609	$C_{12}[^{13}C]_2H_{21}FeN_2O_9$	13.022
426.0495	$C_{12}H_{22}[^{65}Cu]N_2NaO_8$	− 1.38	na			na			na		
nd			415.054	$C_{12}H_{23}FeO_{12}$	0.257	427.0929	$[^{13}C]_{12}H_{23}FeO_{12}$	2.93	415.0516	$C_{12}H_{23}FeO_{12}$	5.525
nd			451.0306	$C_{12}H_{24}[^{35}Cl]FeO_{12}$	0.63	463.0713	$[^{13}C]12H_{24}[^{35}Cl]FeO_{12}$	1.03	451.0283	$C_{12}H_{24}[^{35}Cl]FeO_{12}$	−5.02
nd			453.0294	$C_{12}H_{24}^{[37}Cl]FeO_{12}$	3.94	465.0634	$C_{12}H_{24}[^{37}Cl]FeO_{12}$	− 9.62	453.0289	$C_{12}H_{24}[^{37}Cl]FeO_{12}$	2.84
493.0852	$C_{15}H_{28}[^{63}Cu]NO_{13}$	0.945	486.0917	$C_{15}H_{28}FeNO_{13}$	1.425	498.1289	$C_3[^{13}C]_{12}H_{28}FeNO_{13}$	4.748	487.0918	$C_{14}[^{13}C]H_{28}FeNO_{13}$	5.26
495.0837	$C_{15}H_{28}[^{65}Cu]NO_{13}$	0.321	na			na			na		
475.0761	$C_{15}H_{26}[^{63}Cu]NO_{12}$	2.102	468.0798	$C_{15}H_{26}FeNO_{12}$	0.2	480.116	$C_3[^{13}C]_{12}H_{26}FeNO_{12}$	9.79	nd		
564.121	$C_{18}H_{33}[^{63}Cu]N_2O_{14}$	3.155	557.1295	$C_{18}H_{33}FeN_2O_{14}$	2.475	569.1658	$C_6[^{13}C]_{12}H_{33}FeN_2O_{14}$	4.531	559.1323	$C_{16}[^{13}C]_2H_{33}FeN_2O_{14}$	4.526
566.1197	$C_{18}H_{33}[^{65}Cu]N_2O_{14}$	2.248	na			na			na		

[a] All of the ions listed in Table S1 are included in this table.
[b] Error (in ppm) in calculating the elemental composition.
[c] nd: not detected.
[d] [M + 2] represents copper isotopes 65Cu.
[e] na: not available.
[f] [M + 2] represents chlorine isotopes37Cl

3.1.2.1. MS/MS fragmentations of the Amadori product (m/z 252), the Amadori product-iron complex (m/z 395), and Amadori product of fructosamine (m/z 342) using a collision energy of 10 eV. To further confirm the structures of the glucose/alanine Amadori products, the free ARP, the Amadori product of fructosamine, and the ARP(alaninate)iron(II) complex observed at *m/z* 252, 342, and 395, respectively, were analyzed using ESI/qTOF/MS/MS, and the MS/MS fragmentations are shown in Fig. 1 that the free ARP and the Amadori product of fructosamine formed with glucose generated a greater number of fragment ions under a 10 eV ionization energy compared to the ARP(alaninate)iron(II) complex (*m/z* 395), which generated only four fragment ions, thereby indicating the stability imparted by metal ion complexation to the Amadori product (see Table 4). As shown in Fig. 1, the fragment ions are consistent with the proposed structures, and the MS/MS fragmentations of the free ARP (Fig. 1A) generated the expected diagnostic ions at *m/z* 88 and 97 (Xing et al., 2020) in addition to dehydrated ions at *m/z* 234 and 216 characteristic of the Amadori compounds in positive ionization mode. (Xing et al., 2020).

3.1.3. Detection of amino sugars and their complexes

Amino sugars, such as fructosamine, are known to be formed in Maillard model systems containing metal ions (Nashalian and Yaylayan, 2015). They originate from the oxidative decarboxylation of glucose-conjugated *bis*(amino acid) metal complexes. As expected, fructosamine was observed only in the metal ion containing model systems, and was detected in the form of $[M + H]^+$ at *m/z* 180.0867 ($C_6H_{14}NO_5$) or as $[M + Na]^+$ at *m/z* 202.071 ($C_6H_{13}NNaO_5$). This ion, which is considered to the Amadori product of ammonia, underwent three characteristic dehydration reactions, generating $[M + H - H_2O]^+$ at *m/z* 162.0757 ($C_6H_{12}NO_4$), $[M + H - 2H_2O]^+$ at *m/z* 144.0645 ($C_6H_{10}NO_3$), and $[M + H - 3H_2O]^+$ at *m/z* 126.0543 ($C_6H_8NO_2$). All of the above ions incorporated six carbon atoms from glucose and no C-3 atoms from alanine, further supporting the proposed structures. Furthermore, the Schiff base formed between fructosamine and the Strecker aldehyde of alanine (acetaldehyde) along with its dehydration product were also observed at *m/z* 206.102 ($C_8H_{16}NO_5$) and *m/z* 188.0917 ($C_8H_{14}NO_4$), respectively. In the iron(II)-containing model systems (see Tables 3 and S1), both of the above ions incorporated six carbon atoms from glucose and one C-3 atom from alanine. In addition, the Amadori product formed between fructosamine and glucose was observed at *m/z* 342.14 ($C_{12}H_{24}NO_{10}$), along with its three dehydration products at *m/z* 324.1292 ($C_{12}H_{22}NO_9$), *m/z* 306.1188 ($C_{12}H_{20}NO_8$), and *m/z* 288.107 ($C_{12}H_{18}NO_7$). Moreover, the monohydrated product $[M + H + H_2O]^+$ was also detected at *m/z* 360.1503 ($C_{12}H_{26}NO_{11}$) (Table 3). All the five ions, including the three dehydrated ions and one hydrated ion, were found to incorporate twelve carbon atoms from glucose and no C-3 atoms from alanine.

3.1.4. Detection of iron (II) complexes of sugar degradation products

The formation pathways of the reactive sugar degradation products, such as glyoxal and methylglyoxal have been previously reported in the literature (Kerler et al., 2010a; Hodge, 1953), and these compounds are up to 20,000-fold more reactive than glucose (Hofmann, 1999; Usui et al., 2007). As a result, they have been widely studied in model systems (Marceau and Yaylayan, 2009; Yan et al., 2019; Kerler et al., 2010b; Scalone et al., 2015; Thornalley, 2005; Wang and Ho, 2012); however, the profiling of SDPs is complicated due to their high reactivities and their ability to undergo further reactions prior to detection. In this study,

Table 4
MS/MS fragmentations of the ions observed at *m/z* 252, 342, and 395 generated in the Ala/Glu/$FeCl_2$ model system using 10 eV collision energy (see Fig. 1).

Product ions of *m/z* 252							
Structure	*m/z*	Elemental composition[a]	Error PPM[b]	Glu [^{13}C–U]	Error PPM	Ala [^{13}C-3]	Error PPM
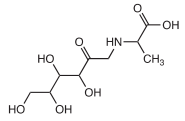 $[M + H]^+ = 252$	88.0386	$C_3H_6NO_2$	– 14.24	0	– 14.24	nd[c]	
	90.0547[d]	$C_3H_8NO_2$	– 8.92	0	– 8.92	1	9.426
	97.028	$C_5H_5O_2$	– 9.84	5	– 6.16	0	– 9.84
	99.0439	$C_5H_7O_2$	– 7.11	Nd		0	– 7.11
	102.0546	$C_4H_8NO_2$	– 8.85	1	8.329	1	7.358
	104.0705	$C_4H_{10}NO_2$	– 6.28	1	– 26.73	1	7.694
	112.0386	$C_3H_7NNaO_2$	10.28	0	– 4.89	1	– 7.10
	126.0546	$C_4H_9NNaO_2$	11.92	Nd		nd	
	146.0804	$C_6H_{12}NO_3$	– 9.02	6	8.2	0	8.34
	168.0651	$C_8H_{10}NO_3$	– 5.76	6	24.72	1	10.332
	216.0866	$C_9H_{14}NO_5$	– 2.77	6	7.774	1	14.68
	234.0984	$C_9H_{16}NO_6$	2.72	6	7.46	1	7.304
Product ions of *m/z* 342							
Structure	***m/z***	**Elemental composition**	**Error PPM[a]**	**Glu [^{13}C–U]**	**Error PPM[a]**	**Ala [^{13}C-3]**	**Error PPM[a]**
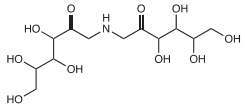 $[M + H]^+ = 342$	90.0548[d]	$C_3H_8NO_2$	– 7.81	3	28.281	0	8.922
	104.0703	$C_4H_{10}NO_2$	– 8.2	nd		0	8.202
	144.0659	$C_6H_{10}NO_3$	– 1.17	6	7.977	0	11.579
	146.0812	$C_6H_{12}NO_3$	– 3.55	6	8.2	0	8.34
	162.0762	$C_6H_{12}NO_4$	– 2.67	6	9.292	0	9.458
	164.0921	$C_6H_{14}NO_4$	– 1.11	6	– 10.06	0	– 10.26
	174.077	$C_7H_{12}NO_4$	2.11	7	– 16.66	0	2.68
	288.1094	$C_{12}H_{18}NO_7$	3.72	12	17.941	0	11.2
	306.1207	$C_{12}H_{20}NO_8$	5.91	12	6.757	0	5.526
	324.1319	$C_{12}H_{22}NO_9$	7.54	12	6.587	0	6.036
	342.1424	$C_{12}H_{24}NO_{10}$	6.95	12	6.717	0	5.615
Product ions of *m/z* 395							
Structure	***m/z***	**Elemental composition**	**Error PPM[a]**	**Glu [^{13}C–U]**	**Error PPM[a]**	**[^{13}C-3] Ala**	**Error PPM[a]**
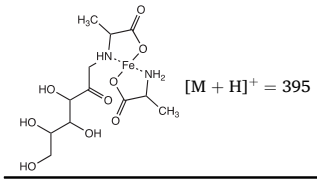 $[M + H]^+ = 395$	90.0552[d]	$C_3H_8NO_2$	– 3.37	0	8.922	1	9.426
	215.9955	$C_6H_{10}FeNO_4$	– 1.94	3	3.148	1	12.81
	246.0074	$C_7H_{12}FeNO_5$	3.72	4	– 7.61	1	– 6.63
	306.0292	$C_9H_{16}FeNO_7$	5.19	6	7.204	1	8.383

[a] All of the ions listed in Figure 1 are included in this table.
[b] Error (in ppm) in calculating the elemental composition.

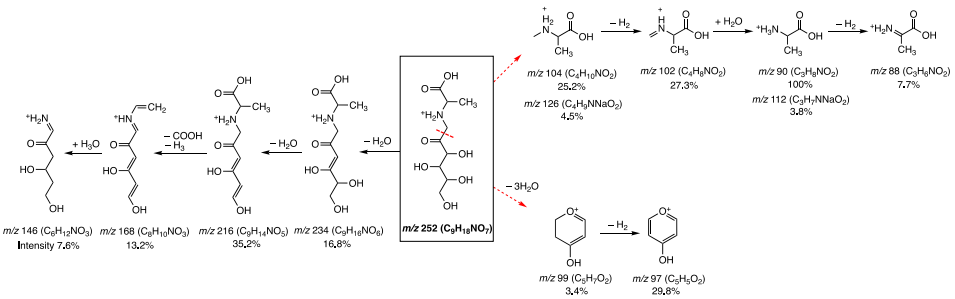

(A) Proposed MS/MS fragmentation pathways of the ions at *m/z* 252

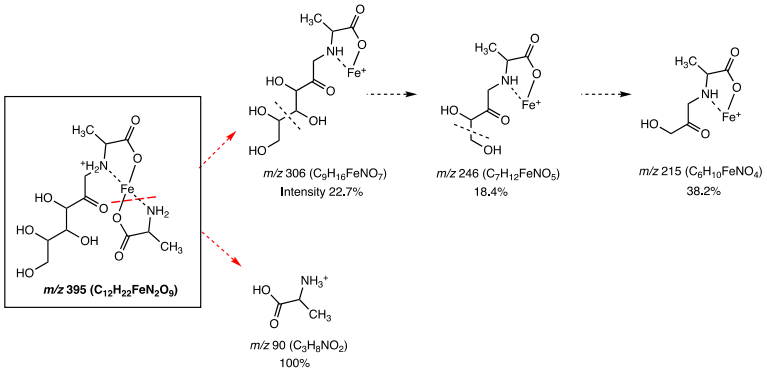

(B) Proposed MS/MS fragmentation pathways of the ions at *m/z* 395

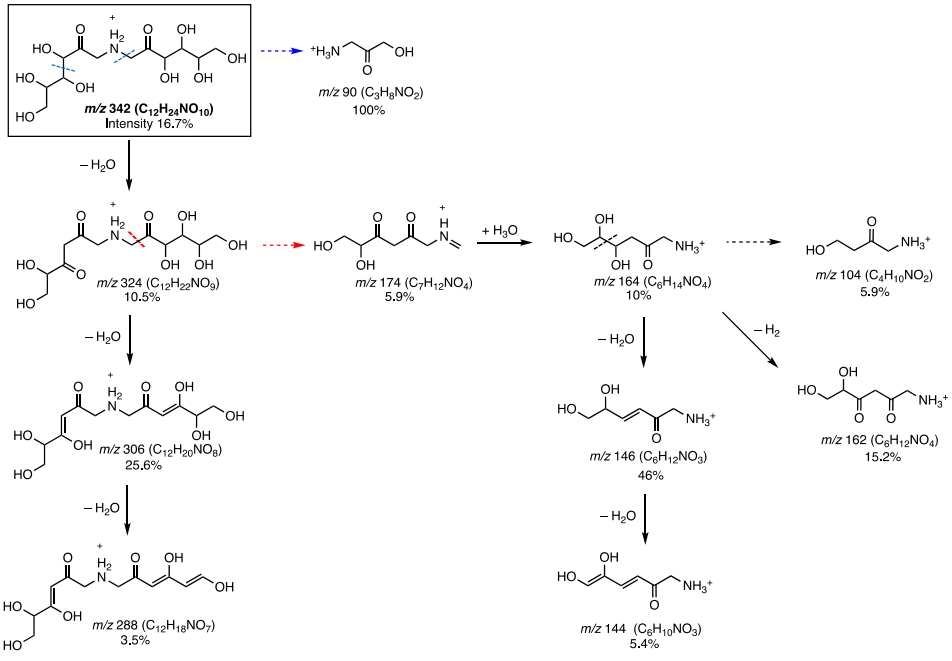

(C) Proposed MS/MS fragmentation pathways of the ions at *m/z* 342

Fig. 1. Proposed MS/MS fragmentation pathways of **(A)** Amadori products (*m/z* 252), **(B)** Amadori product conjugated (alaninate)iron(II) their derivatives (*m/z* 395), and **(C)** glucose conjugated amino sugar (*m/z* 342) in the Ala/Glu/$FeCl_2$ model system.

it was found that these reactive intermediates, when generated in the presence of metal ions, can act as bidentate ligands and be converted into stable metal complexes that can be easily profiled by ESI/qTOF/MS. Furthermore, the ability of various SDPs to undergo self- or random complexation with other SDPs can generate multiple metal-centered binary complexes of the same SDPs; for example, 3-DG was found to form metal complexes with alanine and with itself, thereby providing several opportunities for their identification. In the absence of metal ions, no SDPs were detected due to their high reactivities. A total of 37 degradation products of the MRIs (including their dehydration products) were detected, as confirmed by isotope labelling experiments (see Tables 3 and S2). In this context, alanine was able to form iron(II) complexes with SDPs, such as glycolaldehyde, acetol, glyceraldehyde, 3-deoxyerythrose, and erythrose, which were observed at *m/z* 203.9955 ($C_5H_{10}FeNO_4$), *m/z* 218.011 ($C_6H_{12}FeNO_4$), *m/z* 234.0079 ($C_6H_{12}FeNO_5$), *m/z* 248.0247 ($C_7H_{14}FeNO_5$), and *m/z* 264.0162 ($C_7H_{12}FeNO_6$), respectively. Supporting evidence for these structures were provided by observing the incorporation of expected number of carbon atoms from [^{13}C–U] glucose and [^{13}C-3] alanine. For example, the binary complex of glycolaldehyde with alanine was found to incorporate two carbon atoms from glucose and one C-3 atom from alanine, while acetol and glyceraldehyde complexes incorporated three carbon atoms from glucose, and 3-deoxyerythrose and erythrose complexes incorporated four carbon atoms from glucose with one C-3 atom originating from alanine. Glyceraldehyde and erythrose were also observed as their respective iron(II) complexes. More specifically, the glyceraldehyde complex was detected as $[M]^+$ at *m/z* 144.9585 ($C_3H_5FeO_3$) and erythrose was observed in the form of $[M]^+$, $[M + {}^{35}Cl]^+$, and $[M + {}^{37}Cl]^+$, at *m/z* 174.969 ($C_4H_7FeO_4$), 210.9473 ($C_4H_8[^{35}Cl]FeO_4$), and 212.9434 ($C_4H_8[^{37}Cl]FeO_4$), respectively. All structures were confirmed by detecting the incorporation of expected number of carbon atoms from [^{13}C–U] glucose. For example, glyceraldehyde and erythrose incorporated three and four carbon atoms from [^{13}C–U] glucose, respectively, but no C-3 carbon atom from alanine. Other SDPs, such as dideoxypentosone, erythritol, 3-deoxy-glucoson-5-one, rhamnose, and ribose were also observed as their corresponding iron(II) complexes. Some of these SDPs such as dideoxypentosone and 3-deoxy-glucoson-5-one were associated with solvent molecules, i.e., water or methanol. More specifically, the former was detected in its hydrated form associated with an iron(II) complex to give $[M]^+$ at *m/z* 188.9843 ($C_5H_9FeO_4$), where five carbon atoms from glucose were incorporated, while the latter was observed in its methanolated form complexed with iron(II) to give $[M + Na]^+$ at *m/z* 268.9734 ($C_7H_{10}FeNaO_6$) where six carbon atoms from glucose and no C-3 carbon atoms from alanine were incorporated in the structure. In addition, erythritol was observed as an iron complex with dehydrated erythrosone at *m/z* 295.0113 ($C_8H_{15}FeO_8$). Supporting information was provided by observing the incorporation of eight carbon atoms from [^{13}C–U] glucose (Kim and Yaylayan, 2020). Furthermore, rhamnose was found to form an iron complex with glyceraldehyde and was detected as $[M + H]^+$ at *m/z* 309.0278 ($C_9H_{17}FeO_8$), where nine carbon atoms from glucose was incorporated in the structure. Moreover, pentose was detected as a binary iron(II) complex i.e., $[M + H]^+$ at *m/z* 355.0327 ($C_{10}H_{19}FeO_{10}$), with its dehydrated form $[M + H - H_2O]^+$ at *m/z* 337.0247 ($C_{10}H_{17}FeO_9$). All of the above ions incorporated as expected ten carbon atoms from glucose and no C-3 atoms from alanine (Table S2).

Along with ARP, the 3-DG was also found to be one of the highest intensity peaks, and was associated with solvent molecules (i.e., water and/or methanol) in the forms of $[M + Fe^{35}Cl]^+$, $[M + Fe^{37}Cl]^+$, and $[M + H]^+$ in the Ala/Glu/$FeCl_2$ system. The monohydrated 3-DG iron(II) complex was detected in the form of $[M + Fe^{35}Cl]^+$ at *m/z* 270.9673 ($C_6H_{12}[^{35}Cl]FeO_6$) and $[M + Fe^{37}Cl]^+$ at *m/z* 272.9646 ($C_6H_{12}[^{37}Cl]FeO_6$), and also in the form of $[M + H]^+$ at *m/z* 234.9907 ($C_6H_{11}FeO_6$) (Kim and Yaylayan, 2020). Furthermore, its dehydration peaks were observed as $[M + H - H_2O]^+$ at *m/z* 216.9802 ($C_6H_9FeO_5$) and $[M + H - 2H_2O]^+$ at *m/z* 198.9686 ($C_6H_7FeO_4$) (Table 3). All the five ions corresponding to 3-DG were found to incorporate six carbon atoms form glucose and no carbon atoms from alanine. In addition, 3-DG was detected as a binary iron(II) complex in the form of $[M + Fe^{35}Cl]^+$ at *m/z* 451.0306 ($C_{12}H_{24}[^{35}Cl]FeO_{12}$) and $[M + Fe^{37}Cl]^+$ at *m/z* 453.0294 ($C_{12}H_{24}[^{37}Cl]FeO_{12}$), as well as $[M + H]^+$ at *m/z* 415.054 ($C_{12}H_{23}FeO_{12}$). These structures were found to incorporate twelve carbon atoms from glucose, but no carbon atoms from alanine. Furthermore, 3-DG was also detected as methanolated iron(II) complex corresponding to $[M + Fe^{35}Cl]^+$ at *m/z* 284.9825 ($C_7H_{14}[^{35}Cl]FeO_6$) and $[M + Fe^{37}Cl]^+$ at *m/z* 286.9816 ($C_7H_{14}[^{37}Cl]FeO_6$). These hydrated- and methanolated 3-DG iron(II) complexes were confirmed based on their MS/MS fragmentations (Kim and Yaylayan, 2020), and by observing the incorporation of six carbon atoms from glucose. Moreover, Hydroxymethylfurfural (HMF) was detected as $[M + H]^+$ at *m/z* 127.0389 ($C_6H_7O_3$); both in the presence and absence of iron(II). The peak intensity of HMF in the Ala/Glu/$FeCl_2$ system was at least 2-fold higher than in the Ala/Glu model system (Table 3). As expected, the ion observed at *m/z* 127.0389 incorporated six carbon atoms from glucose. Finally, 3-DG was detected also as alanine-iron(II) complex $[M + H]^+$ at *m/z* 306.0274 ($C_9H_{16}FeNO_7$), in addition to its corresponding dehydrated product $[M + H - H_2O]^+$ at *m/z* 288.0174 ($C_9H_{14}FeNO_6$) and $[M + H - 2H_2O]^+$ at *m/z* 270.0067 ($C_9H_{12}FeNO_5$). Furthermore, 3-DG conjugated with mono(alaninato) iron(II) was also observed at *m/z* 342.0044 and *m/z* 344.0026, corresponding to $[M + Fe^{35}Cl]^+$ ($C_9H_{17}Fe[^{35}Cl]NO_7$) and $[M + Fe^{37}Cl]^+$ ($C_9H_{17}Fe[^{37}Cl]NO_7$), respectively (Table S2). All the five ions corresponding to 3-DG conjugated with mono(alaninate)iron(II) were found to incorporate six carbon atoms from glucose and one C-3 carbon atom from alanine.

4. Conclusions

The addition of metal ions to Maillard model systems before heating not only enhances the reaction and generates metal specific products, such as fructosamine, but also stabilizes many of the reactive enediol-containing moieties through the formation of binary metal complexes, which renders them easily detectable by electrospray ionization/quadrupole time-of-flight mass spectrometry (ESI/qTOF/MS).

CRediT authorship contribution statement

Eun Sil Kim: Data curation, Formal analysis, Methodology, Validation, and, Writing – original draft. **Varoujan Yaylayan:** Supervision, Conceptualization, Project administration, Writing – review & editing, and, Funding acquisition.

Declaration of competing interest

The authors declare no conflict of interest.

Acknowledgements

The authors acknowledge funding for this research from Natural Sciences and Engineering Research Council of Canada (NSERC) and McGill University.

Appendix A. Supplementary data

Supplementary data to this article can be found online at https://doi.org/10.1016/j.crfs.2021.04.003.

References

Davidek, T., Clety, N., Aubin, S., Blank, I., 2002. Degradation of the Amadori compound *N*-(1-Deoxy-D-frutos-1-yl)glycine in aqueous model systems. J. Agric. Food Chem. 50, 5472–5479. https://doi.org/10.1021/jf025561j.

Gensberger, S., Glomb, M.A., Pischetsrider, M., 2013. Analysis of sugar degradation products with α-dicarbonyl structure in carbonated soft drinks by UHPLC-DAD-MS/

MS. J. Agric. Food Chem. 61 (43), 10238–10245. https://doi.org/10.1021/jf3048466.
Hodge, J.E., 1953. Chemistry of browning reactions in model systems. J. Agric. Food Chem. 1 (15), 928–943. https://doi.org/10.1021/jf60015a004.
Hofmann, T., 1999. Quantitative studies on the role of browning precursors in the Maillard reaction of pentoses and hexoses with L-alanine. Eur. Food Res. Technol. 209, 113–121. https://doi.org/10.1007/s002170050468.
Kaufmann, M., Meissner, P.M., Pelke, D., Mügge, C., Kroh, L.W., 2016. Structure–reactivity relationship of *Amadori* rearrangement products compared to related ketoses. Carbohydr. Res. 428 (16), 87–99. https://doi.org/10.1016/j.carres.2016.04.016.
Kerler, J., Winkel, C., Davidek, T., Blank, I., Food Flavour Technology, 2010. Basic chemistry and process conditions for reaction flavours with particular focus on Maillard-type reactions. In: Taylor, A.J., Linforth, S.T. (Eds.), John Wiley & Sons, Wiley-Blackwell, pp. 51–88.
Kerler, J., Winkel, C., Davidek, T., Blank, I., Food Flavour Technology, 2010. Basic chemistry and process conditions for reaction flavours with particular focus on Maillard-type reactions. In: Taylor, A.J., Linforth, S.T. (Eds.), John Wiley & Sons, Wiley-Blackwell, pp. 51–88.
Kim, E.S., Yaylayan, V., 2020. Profiling of sugar degradation products through Complexation with Divalent Metal ions coupled with ESI/qTOF/MS/MS analysis. Curr. Res. Food Sci. 3, 268–274. https://doi.org/10.1016/j.crfs.2020.10.001.
Li, C., Wang, H., Juárez, M., Ruan, E.D., 2014. Structural characterization of Amadori rearrangement product of glucosylated Nα-acetyl-lysine by nuclear magnetic resonance spectroscopy. Int. J. Spectrosc. 1–6. https://doi.org/10.1155/2014/789356.
Marceau, E., Yaylayan, V.A., 2009. Profiling of a-dicarbonyl content of commercial honeys from different botanical origins: identification of 3,4-Dideoxyglucosone-3-ene (3,4-DGE) and related compounds. J. Agric. Food Chem. 57, 10837–10844. https://doi.org/10.1021/jf903341t.
Nashalian, O., Yaylayan, V.A., 2015. Sugar-conjugated bis(glycinato)copper (II) complexes and their modulating influence on the maillard reaction. J. Agric. Food Chem. 63, 4353–4360. https://doi.org/10.1021/acs.jafc.5b00932.
Page, B.D., Conacher, B.S., 1982. The pros and cons of derivatization in the chromatographic determination of food additives. In: Frei, R.W. (Ed.), Chemical Derivatization in Analytical Chemistry. Springer, US, pp. 243–292.
Patiny, L., Borel, A. ChemCals, 2013. A building block for tomorrow's chemical infrastructure. J. Chem. Inf. Model. 53 (5), 1223–1228. https://doi.org/10.1021/ci300563h.
Scalone, G.L.L., Cucu, T., Kimpe, N.D., Meulenaer, B.D., 2015. Influence of free amino acids, oligopeptides, and polypeptides on the formation of pyrazines in maillard model systems. J. Agric. Food Chem. 63 (22), 5364–5373. https://doi.org/10.1021/acs.jafc.5b01129.
Tamic, L.A., Hartman, K.A., 1983. The infrared spectra and structure of the Amadori product formed from glucose and Glycine. Appl. Spectrosc. 39 (4), 591–594.
Thornalley, P.J., 2005. Dicarbonyl intermediates in the maillard reaction. N. Y. Acad. of Sci. 1043, 111–117. https://doi.org/10.1196/annals.1333.014.
Usui, T., Yanagisawa, S., Ohguchi, M., Yoshino, M., Kawabata, R., Kishimoto, J., Arai, Y., Watanabe, H., Hayase, F., 2007. Identification and determination of a-dicarbonyl compounds formed in the degradation of sugars. Biosci. Biotech. Bioche. 71 (10), 2465–2472. https://doi.org/10.1271/bbb.70229.
Wang, Y., Ho, C.T., 2012. Flavour chemistry of methylglyoxal and glyoxal. Chem. Soc. Rev. 41, 4140–4149. https://doi.org/10.1039/C2CS35025D.
Wnorowski, A., Yaylayan, V.A., 2003. Monitoring carbonyl-amine reaction between pyruvic acid and α-amino alcohols by FTIR spectroscopy-A possible route to Amadori products. J. Agric. Food Chem. 51 (22), 6537–6543. https://doi.org/10.1021/jf034581y.
Xing, H., Mossine, V.V., Yaylayan, V., 2020. Diagnostic MS/MS fragmentation patterns for the discrimination between Schiff bases and their Amadori or Heyns rearrangement products. Carbohydr. Res. 491, 107985. https://doi.org/10.1016/j.carres.2020.107985, 107985.
Yan, S., Sun, M., Zhao, L., Wang, K., Fang, X., Wu, L., Xue, X., 2019. Comparison of differences of a-dicarbonyl compounds between Naturally matured and artificially heated Acacia honey: their application to determine honey quality. J. Agric. Food Chem. 67 (46), 12885–12894. https://doi.org/10.1021/acs.jafc.9b05484.
Yaylayan, V.A., 1997. Classification of the Maillard reaction: a conceptual approach. Trends Food Sci. Technol. 8, 13–18. https://doi.org/10.1016/S0924-2244(96)20013-5.
Yaylayan, V.A., Huyghues-Despointes, A., 1994. Chemistry of Amadori rearrangement products: analysis, synthesis, kinetics, reactions, and spectroscopic properties. Crit. Rev. Food Sci. Nutr. 34 (4), 321–369. https://doi.org/10.1080/10408399409527667.